

## Rb-stabilized laser at 1572 nm for CO<sub>2</sub> monitoring

**R Matthey, W Moreno, F Gruet, P Brochard, S Schilt and G Miletì**

Laboratoire Temps-Fréquence, Institut de Physique,  
Université de Neuchâtel, Neuchâtel, Switzerland

E-mail: renaud.matthey-de-lendroit@unine.ch

**Abstract.** We have developed a compact rubidium-stabilized laser system to serve as optical frequency reference in the 1.55- $\mu\text{m}$  wavelength region, in particular for CO<sub>2</sub> monitoring at 1572 nm. The light of a fiber-pigtailed distributed feedback (DFB) laser emitting at 1560 nm is frequency-doubled and locked to a sub-Doppler rubidium transition at 780 nm using a 2-cm long vapor glass cell. Part of the DFB laser light is modulated with an electro-optical modulator enclosed in a Fabry-Perot cavity, generating an optical frequency comb with spectral coverage extending from 1540 nm to 1580 nm. A second slave DFB laser emitting at 1572 nm and offset-locked to one line of the frequency comb shows a relative frequency stability of  $1 \cdot 10^{-11}$  at 1 s averaging time and  $<4 \cdot 10^{-12}$  from 1 hour up to 3 days.

### 1. Introduction

Some applications require a frequency-stable laser source operating at a precise wavelength where no direct suitable molecular or atomic reference transition exists. A reason may be the weakness of the considered transition line-strength that would require long optical interaction length to ensure a sufficient absorption signal for laser stabilization. In other cases, the laser must precisely emit at a frequency lying on the wing of an absorption line, at a detuning of up to several GHz from the line center, or even out of any absorption line. An example of such application is the measurement of the concentration of carbon dioxide (CO<sub>2</sub>) in the atmosphere based on the integrated-path differential-absorption lidar (IPDA) technique [1], as envisaged by space agencies [2] to identify on a global scale and more precisely the CO<sub>2</sub> exchanges between the atmosphere and the Earth's lands and oceans [3]. The constraints imposed on the lidar instrument for a CO<sub>2</sub> mission were defined by feasibility studies [3, 4]. For a transmitter laser emitting at 1572 nm, on the slope of a CO<sub>2</sub> absorption line, a frequency stability – in terms of Allan deviation – below 20 kHz ( $<10^{-10}$  fractional frequency stability) is requested for integration times from 700 s up to 3 years of mission operation time [5].

A relative frequency stability of about  $3 \cdot 10^{-11}$  was demonstrated by Numata *et al.* for integration time up to 1,000 s at a wavelength of 1572.34 nm [6]. In this case, a distributed feedback (DFB) laser diode was frequency-stabilized at the center of a Doppler-broadened CO<sub>2</sub> line using a multipass cell with a path-length of 17 m combined with a laser frequency modulation technique. In the implemented approach, additional lasers could be offset-locked up to  $\pm 7$  GHz away from the master laser. Besides, compact 780-nm Rb-based frequency-stabilized laser heads were previously developed in our premises for atomic clocks, using DFB lasers and evacuated Rb cells with an optical path-length of a few centimeters only. These laser heads show a relative frequency stability better than  $1 \cdot 10^{-11}$  at all time-scales between 1 s and 1 day [7]. The main goal of the present work consisted in transferring the high frequency stability achievable with an Rb cell to an arbitrary wavelength in the 1.55- $\mu\text{m}$  wavelength region, in particular around 1572 nm, for CO<sub>2</sub> monitoring purpose.



The laser system is illustrated in Figure 1. A fiber-pigtailed DFB laser emitting at 1560 nm (master laser) is frequency-doubled and stabilized to the D<sub>2</sub> line of <sup>87</sup>Rb at 780 nm. A part of the master laser light is injected into an electro-optical modulator (EOM) enclosed in a Fabry-Perot cavity to generate an optical frequency comb (OFC). A second DFB laser emitting at 1572 nm (slave laser) is offset-locked to one line of the generated comb. The output of the system consists of a fraction of the stabilized slave laser light. The optical system is fully fibered.

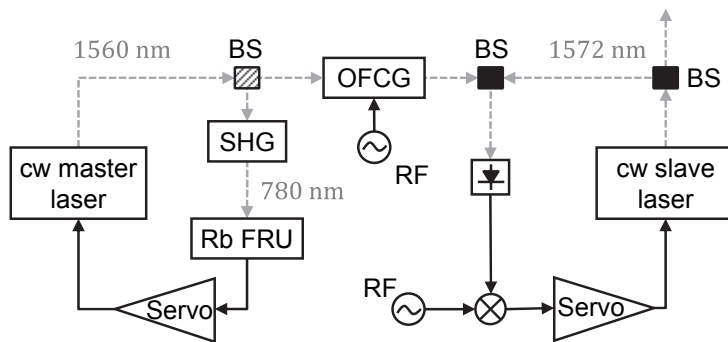


**Figure 1.** Schematics of the laser system. Dashed grey lines and black lines correspond to optical fibers and electrical links, respectively. BS: beam splitter (hatched one: see text); OFCG: optical frequency comb generator; Rb FRU: rubidium frequency reference unit; RF: radio frequency oscillator; SHG: second harmonic generator.

## 2. Experimental Setup

### 2.1. Frequency Doubling for Stabilization at 1560 nm

The master laser is a fiber-pigtailed DFB laser (Emcore) emitting up to 80 mW of optical power at 1560 nm. The laser has a full width at half-maximum (FWHM) linewidth of 1-2 MHz (at 4-ms observation time), determined using the concept of the  $\beta$ -separation line [8] from its measured frequency noise spectrum and also from the recorded beat note with two independent lasers. A fibered optical isolator is disposed at the output of the master laser to prevent unwanted feedback. A 50/50 polarization-maintaining fiber beam splitter (PM-BS) splits the light into two outputs; the first one is used for frequency stabilization and the second to generate the OFC.

The first output of the PM-BS is frequency-doubled using a second harmonic generator (SHG) module made of a fiber-pigtailed 5-cm-long periodically-poled lithium niobate (PPLN) waveguide. The optimal operation temperature and the efficiency of the module were determined to be 50°C and 300 %/W (including the fiber coupling losses), respectively [9]. The frequency-doubled light is then injected into a frequency reference unit (FRU) that has a similar design as the one integrated in the laser heads described by Gruet *et al.* [7]. There, it optically pumps the <sup>87</sup>Rb atoms (D<sub>2</sub> line, 780.24 nm) contained in a home-built evacuated cylindrical cell (10-mm diameter by 19-mm length). The cell is thermalized and mounted in a magnetically-shielded package. The light is retro-reflected in order to probe the Rb vapor in a sub-Doppler absorption scheme that provides narrow resonances (~15 MHz FWHM) for frequency-locking.

Frequency-stabilization of the master laser is achieved by modulating its injection current with a 50-kHz sinusoidal signal and applying synchronous demodulation of the detected light intensity at the first harmonic of the modulation frequency. The correction signal obtained after a proportional-integrator servo-controller is applied to the laser current in a feedback loop.

### 2.2. Optical Frequency Comb Generation

The frequency-stabilized master laser is used to seed an OFC generator (OptoComb). The injected light is phase-modulated by an EOM enclosed in a waveguide Fabry-Perot cavity with a finesse of 60 and a free spectral range of 2.5 GHz. The EOM is driven by a radio-frequency (RF) signal in resonance with the cavity at the fourth harmonic of its free-spectral range, i.e., 10 GHz, to enhance the efficiency of the sideband generation process. Hence, a widely-spanning frequency comb is generated with a spectral coverage of 40 nm centred at the master laser frequency (Figure 2). The synthesizer generating the RF signal applied to the EOM is referenced to a hydrogen maser for long-term stability.

By denoting  $f_m$  and  $\nu_M$  the RF and master laser frequency, respectively, the frequency of the  $n$ th-order optical comb line,  $\nu_n$ , is given by  $\nu_n = \nu_M + n \cdot f_m$ , where  $n$  can take a positive or negative integer value. As the frequency stability of the RF signal considerably exceeds that of the master laser, the frequency of all comb modes follows the fluctuations of the master laser. The frequency dithering applied to stabilize the master laser is thus also transferred to each mode of the frequency comb, which gives the possibility to offset-lock a slave laser to one mode of the comb without requiring any further frequency modulation, e.g., of the slave laser.

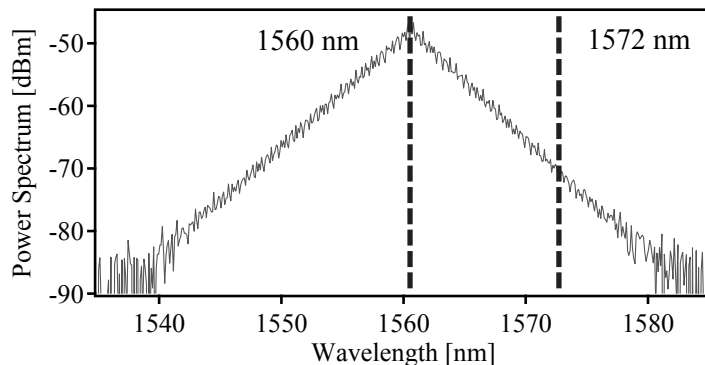


**Figure 2.** Spectral envelope of the optical frequency comb covering a span larger than 40 nm around the seed central line of 1560.48 nm, as obtained when driving the EOM at 10 GHz.

### 2.3. Offset-Locking for Stabilization at 1572 nm

For the slave laser, a linewidth of 1-2 MHz (FWHM) was determined in the same way as for the master laser. An optical isolator is disposed at the laser output and a 50/50 PM-BS divides the optical power into two parts. One part constitutes the optical output of the system, while the other is used to offset-lock the slave laser to one mode of the optical frequency comb using a similar method as proposed by Schilt *et al.* [10]. For this purpose, a fast photodiode detects the beat note between the slave laser and the nearest comb mode. After amplification, the beat signal is frequency down-converted by mixing with a local oscillator of frequency  $f_{LO}$  referenced to the same hydrogen maser. The resulting intermediate frequency signal is further filtered using the combination of a 1-MHz high-pass filter and an 11-MHz low-pass filter. Finally, an envelope detector measures the power of the transmitted RF signal, which, after demodulation at the master laser modulation frequency, provides a voltage error signal for an offset-locking stabilization loop [10]. The combination of the filters and envelope detector acts as a frequency discriminator and creates an absorption-like feature in the low-frequency electrical domain (see Figure 3). The frequency down-converted beat note between the slave laser and the comb line can thus be locked to the centre of this feature by generating a derivative-like signal using the dithering of the beat signal that results from the modulation of the master laser. The absence of dithering of the slave laser frequency is beneficial for the injection seeding process of the power oscillator of a lidar transmitter or to serve as an unmodulated optical frequency reference.

The comb line and the offset frequency are selected so that the slave laser emits at the desired frequency  $\nu_s = \nu_M + n \cdot f_m \pm f_{LO}$ . The sign of the offset frequency is determined from the observed change in the injection current of the locked slave laser in response to a variation of the offset frequency  $f_{LO}$ . The mode number  $n$  can be determined when varying the EOM drive frequency  $f_m$  or using an optical spectrum analyser.

## 3. Frequency Stability Results

The frequency stability of the laser system was evaluated at the main stages of the setup, corresponding to different wavelengths, using heterodyne detection with external optical frequency references. Hence, we were able to follow how the stability of the Rb reference is transferred to the slave laser by successively evaluating the master laser before (1560 nm) and after (780 nm) the frequency-doubling process, an optical comb mode (1557 nm) and at last the slave laser (1572 nm).

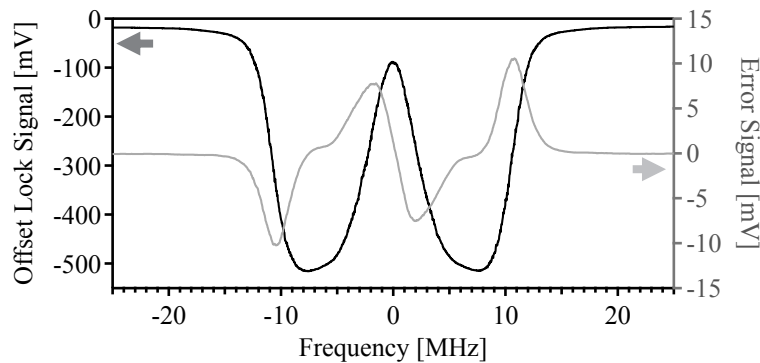


**Figure 3.** Black line: offset-locking signal measured at the output of the envelope detector. Grey line: error signal obtained after demodulation.

### 3.1. Master Laser

The frequency stability of the master laser was measured at 1560 nm and 780 nm. At 1560 nm, a beat note was performed between the master laser locked onto the Rb direct F2→F'3 transition (which is the most stable at long term due to its lower temperature sensitivity [8]) and a self-referenced commercial Er-fiber comb fully stabilized to an H-maser. At 780 nm, the frequency-doubled master laser was heterodyned with an external Rb-stabilized reference laser head locked onto the cross-over CO22/23 transition, which demonstrated relative frequency stability better than  $1 \cdot 10^{-11}$  at all time-scales from 1 s up to 1 day [7]. The measurements of the master laser at 780 nm and 1560 nm were carried out simultaneously – although they did not always have the same overall duration – and for two different types of fiber splitters at the laser output (hatched splitter in Figure 1).

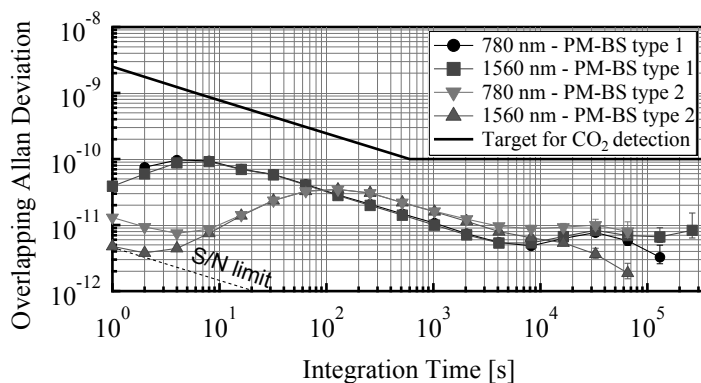


**Figure 4.** Fractional frequency stability of the beat note between the master laser (1560 nm) and the self-referenced comb (■, ▲), and between the frequency-doubled master laser (780 nm) and an external Rb-stabilized reference laser head (●, ▼). (■, ●), (▲, ▼): simultaneous measurement done with the first and second type of PM-BS, respectively.

As presented in Figure 4, a fractional frequency stability of  $5.2 \cdot 10^{-12}$  at 1-s averaging time (corresponding to  $<1$  kHz absolute instability at 1560 nm) is reached with the second type of fiber splitter. This value matches the estimated signal-to-noise limit at 1 s. Above 4,000 s, the long-term relative instability is always lower than  $1 \cdot 10^{-11}$  (2 kHz absolute frequency at 1560 nm). All stability measurements performed at 780 nm were limited by the resolution of the frequency counter, which type and settings differed from the ones used at 1560 nm. This effect is responsible for the difference observed at short term between the results at 780 nm and 1560 nm. The long-term fractional frequency stability at 780 nm is also further limited slightly below  $1 \cdot 10^{-11}$  by the reference laser head for integration times longer than  $10^4$  s.

The first type of fiber splitter induced spurious reflections and associated etalon fringes that degraded the short-term stability at the level of  $1 \cdot 10^{-10}$  at 5 s. The replacement of this low-performing splitter with a better one (type 2 in Figure 4) drastically improved the short-term stability by more than an order of magnitude. With the second type of splitter a previously hidden instability bump reaching  $3 \cdot 10^{-11}$  at around 100-s integration time is observed. It is caused by the presence of a fiber splice at the output of the frequency-doubling module that induces etalon interferences.

### 3.2. Optical Frequency Comb

When the first type of splitter was installed to split the emission of the master laser, the frequency stability of the generated OFC was retrieved from the beat-note frequency measured between one line of the comb and a narrow-linewidth (<10 kHz) auxiliary semiconductor laser operating at 1557 nm. The laser was phase-locked to the self-referenced comb to ensure its long-term frequency stability. The low optical power per mode in the two combs prevented the direct beating of the generated OFC against the self-referenced comb. As shown in Figure 5, the stability of the OFC line at 1557 nm faithfully reproduces the master laser stability at 1560 nm – already presented in Figure 4 but replicated for comparison purpose. The non-concomitance of both measurements results in slight short- and mid-term differences due to modified temperature-induced etalon fringes in the master laser locking loop, and in variations in the long term due to the slowly fluctuating laboratory background temperature.

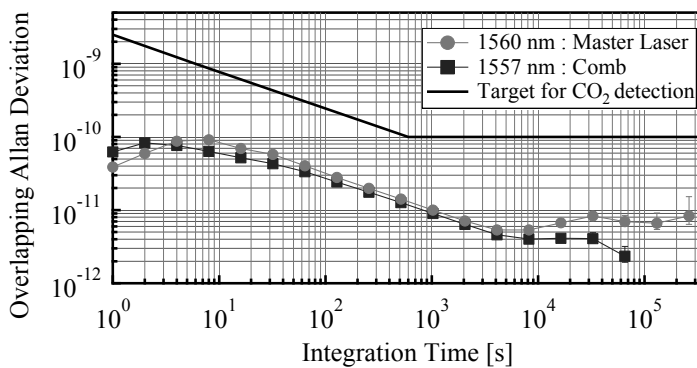


**Figure 5.** Fractional frequency stability of the beat note between one line of the OFC and a 1557-nm auxiliary laser, phase-locked to a self-referenced comb (■), and between the master laser and the self-referenced comb (●). Measurements were not carried out simultaneously.

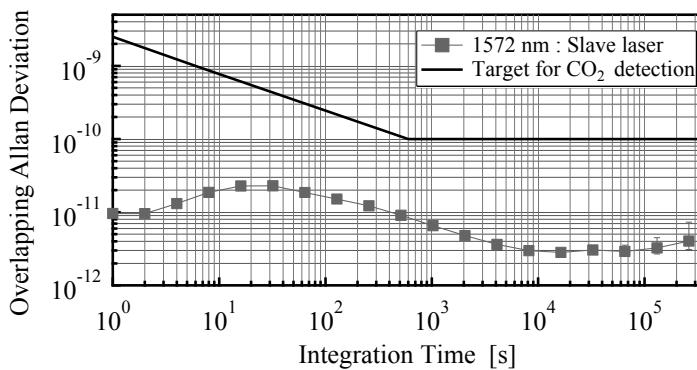


**Figure 6.** Fractional frequency stability of the beat note between the slave laser at 1572 nm and the self-referenced comb (■).

### 3.3. Slave Laser

In the same manner as applied to the master laser, the frequency stability of the slave laser was determined from the beat note with the self-referenced comb fully-stabilized to the H-maser. The offset frequency  $f_{LO}$  in the slave laser stabilization loop was set to 50 MHz and the drive frequency of the OFC generator was chosen so that the slave laser was lying at the center of the CO<sub>2</sub> R20 absorption line (190,743,066.5 MHz). To properly stabilize the slave laser, the modulation amplitude of the master laser, still locked to the direct transition F2→F'3 with the fiber splitter of the second type, was increased, implying a degradation of the short-term stability of the slave laser with respect to the master laser stability previously reported in Figure 4.

The obtained fractional frequency stability of the slave laser is displayed in Figure 6. It amounts to  $1 \cdot 10^{-11}$  at 1 s and stays below  $2.5 \cdot 10^{-11}$  for all timescales up to the maximum assessed integration time of 3 days, reaching  $4 \cdot 10^{-12}$  on the long term. The target stability for atmospheric CO<sub>2</sub> monitoring is by far fulfilled. The measurement was performed under environmental temperature conditions that were different from those prevailing for the evaluation of the master laser stability (see Figure 4). The setup was less protected against rapid temperature changes, which made the temporal frequency fluctuations linked to etalon-like cavity more severe. This resulted in a shift of the instability bump in the Allan deviation towards shorter integration times (~30 s).

#### 4. Discussion and Perspective

For the demonstration of the developed scheme, an H-maser was employed as a frequency reference for the OFC generator driving signal as well as for the offset-locking frequency. Both RFs can be referenced to a more compact and transportable frequency reference such as a commercially-available GPS-referenced Rb atomic clock that offers a sufficient stability compatible with the RF requirements of the system (fractional frequency stability of  $1 \cdot 10^{-9}$ ). Depending on the desired output wavelength, the mixer and RF oscillator of the offset-locking loop might be omitted, locking the slave laser directly to the optical comb and fine-tuning its frequency with the OFC generator modulation frequency.

The accuracy and stability of the output frequency at 1572 nm are most of all dictated by the performance of the master laser as the RF sources used in the setup are much more stable. The accuracy and reproducibility of the master laser frequency, which depend on the selected reference sub-Doppler Rb line and on the frequency stabilization method, are presently being investigated. Our preliminary results suggest that for the direct  $F2 \rightarrow F'3$  transition an accuracy below 100 kHz and a reproducibility of 20 kHz could be reached with a relatively simple and compact rubidium cell setup, in accordance with the results of Ye *et al.* [11].

At present, an imperfection in the fiber at the frequency-doubling module output that induces etalon-like cavities limits the frequency stability of our system between 10-s and 100-s integration time. The reduction of these etalon-like effects should decrease the short-term instability down to the estimated signal-to-noise limit of the master laser ( $5.2 \cdot 10^{-12} \tau^{-1/2}$ ).

#### 5. Conclusion

We have demonstrated that the stability of a DFB laser emitting at 1560 nm, stabilized to rubidium using frequency-doubling and sub-Doppler spectroscopy, can be transferred through the generation of an optical frequency comb and a frequency offset-locking scheme to a second DFB laser emitting at 1572 nm. The relative frequency stability of the master laser is  $5.2 \cdot 10^{-12}$  at 1 s, at the limit of the signal-to-noise. At 1572 nm, a relative frequency stability of  $1 \cdot 10^{-11}$  at 1 s has been obtained, and lower than  $2.5 \cdot 10^{-11}$  for all assessed timescales (1 s to 3 days), reaching  $4 \cdot 10^{-12}$  above 3,000 s. Such result fulfils the requirements for a CO<sub>2</sub> satellite lidar mission. The applied method is not restricted to 1572 nm and can be implemented for any wavelength located within the comb span.

#### 6. Acknowledgement

This work was supported by the European Space Agency and the Swiss National Science Foundation (project number 156621). We thank our colleague Dr. Christoph Affolderbach and Dr. Andreas Fix (DLR, Germany) for helpful discussions.

#### References

- [1] Ehret G, Kiemle C, Wirth M, Amediak A, Fix A and Houweling S 2008 *Appl. Phys. B* **90**, 593
- [2] ESA 2008 *Report for Assessment*, SP-1313/1
- [3] Bréon F M and Ciais P 2009 *Comput. Geosci.* **342** 412
- [4] Caron J, Durand Y, Bezy J L and Meynard R 2009 *Proc. Lidar Technologies Techniques and Measurements for Atmospheric Remote Sensing V* (SPIE, 2009), paper 74790E
- [5] Fix A, Matthey R, Amediak A, Ehret G, Gruet F, Kiemle C, Klein V, Mileti G, Pereira do Carmo J and Quatrevalet M 2014 *Proc. Int. Conf. on Space Optics (Tenerife)*, session 2C
- [6] Numata K, Chen J, Wu S, Abshire J and Krainak M 2011 *Appl. Opt.* **50** 1047
- [7] Gruet F, Pellaton M, Affolderbach C, Bandi T, Matthey R and Mileti G 2012 *Proc. of the Int. Conf. in Space Optics (Ajaccio)*, paper 048
- [8] Di Domenico G, Schilt S and Thomann P 2010 *Appl. Opt.* **49** 4801
- [9] Matthey R, Gruet F, Schilt S and Mileti G 2015 *Opt. Lett.* **40** 2576
- [10] Schilt S, Matthey R, Kauffmann D, Affolderbach C, Mileti G and Thévenaz L 2008 *Appl. Opt.* **47**, 4336
- [11] Ye J, Swartz S, Jungner P and Hall J 1996 *Opt. Lett.* **21** 1280